Latin American Journal of Solids and Structures
www.lajss.org

A Comparative Study on Propagation of Elastic Waves in Random Particulate Composites

Abstract

This paper aims to conduct a comparative study on four different models of effective field and effective medium for modeling propagation of plane elastic waves through the composites containing spherical particles with random distribution. Effective elastic properties along with the normalized phase velocity and attenuation of the average wave was numerically evaluated by the models. The plane incident wave was considered longitudinal to get the results. The numerical analyses were performed on four types of composites in the range of low to intermediate frequency and different volume fractions. Judgment about this comparative study is done based on physical and theoretical concepts in the wave propagation phenomenon. The obtained results provide a good viewpoint in using different models for studying propagation of the plane elastic waves in various particulate composites.

Keywords

Particulate composite, Random media, Wave propagation, Spherical inclusion.

Mohammad Rahimzadeh[a,*]
Kamran Daneshjoo[b]

[a]PhD Student, School of Mechanical Engineering, Iran University of Science and Technology, Tehran, Iran,
[b]Professor, School of Mechanical Engineering, Iran University of Science and Technology, Tehran, Iran, P.O.B. 1684613114

*Author email: mh.rahimzadeh@gmail.com

1 INTRODUCTION

Composite materials have found numerous applications in various industries. These materials have become interesting because their elastic and strength properties can be designed for different loading conditions and because they reduce weight of the structure considerably. Although fibrous composites have marvelous advantages over other composite materials, their rather expensive costs have led to look for other types of materials including particulate composites (Kamat et al. 1989). Major use of these materials can be found in aerospace structures such as commercial and military aircrafts as well as spacecrafts. Identification of the propagation behavior of the elastic waves in these composites will contribute to detect cracks and defects by non-destructive tests.

Propagation of waves in heterogeneous media causes scattering such that makes phase velocity and attenuation of the coherent wave frequency-dependent. Final dynamic response of the medium

can be given by a complex wave number which indicates propagation of the coherent wave in the equivalent homogeneous medium.

Foldy (1945) and Lax (1951) investigated multiple scattering of the waves from point scatterers.They estimated the complex wave number of the coherent wave based on volume fraction of the particles and forward far field scattering amplitude in a single particle wave scattering problem. The achievements of these researchers were further improved by Waterman & Truell (1961). Backward scattering amplitude and forward amplitude in the single scattering problem have been used in the proposed approach to estimate the behavior of multiple scattering.

Lloyd and Berry (1967) developed the recent model and demonstrated that the extracted equations of Waterman-Truell bear an integration error. They found the wave number of the heterogeneous medium by using the approach of energy density. Their final equations contained an additional integral term in comparison with the model of Waterman-Truell and provided somewhat more reliable results in many systems.

There are various contributions based on the abovementioned models for studying the effects of interfaces. Datta et al. (1988) analyzed propagation of plane longitudinal and shear waves in composites containing random distribution of spherical inclusions via Foldy's theory. Sato & Shindo (2003) examined multiple scattering of longitudinal and shear elastic waves in a composite with randomly distributed particles with graded interfacial layers. The effects of viscoelastic interphase on dynamic properties of these composites were studied by Wei and Haung (2004). The numerical results reveal that viscosity of the interface has a noticeable effect on effective elastic modules and effective wave number. They also showed that the dissipation effect of interphase is the biggest at the low frequency range, while the effect of multiple scattering becomes dominant at the high frequency range.

These methods show an acceptable accuracy in modeling the multiple scattering phenomena at small particles volume fractions and low frequency regime. However, it should be noted that these methods do not offer a good estimation of the final static specifications of a heterogeneous medium at zero frequency range. Thus, it is rather impossible to guarantee accuracy of their results at low frequencies.

Varadan et al. (1982, 1985) developed T-Matrix method in multiple scattering of the waves using quasi-crystalline estimations and introducing a pair-correlation function. A similar work was launched by Mal & Bose (1974) who analytically studied the scattering of the plane wave by spherical elastic inclusions which were randomly distributed within an infinite matrix. They found propagation characteristics of the average wave based on a statistical approach by introducing of a pair-correlation function and quasi-crystalline approximation. The effect of imperfect bonding between spherical particles and medium of the surrounding matrix has been investigated during this work. Finding the correlation function between inclusions in multiple scattering of the waves in two-phase media has been subject of studies. Some examples in this regard are the research works conducted by Marco and Willis (1998) Marco (1999) and Liu (2008). Willis (1980) formulated the scattering problems in elastodynamics in terms of integral equations. Finding the pair-correlation function for dense media is one difficulty of the abovementioned methods. The effective elastic constants in these cases will be completely dependent on how these functions are determined.

Berryman (1980) derived effective static properties using elastic wave scattering theory. His solution was set the scattered field equal to zero in order to finding the effective properties. The obtained results demonstrated that this method has a higher accuracy than the one developed by Kuster & Toksoz (1974). The resultant accuracy of this approach is compared with that of other static self-consistent models such as Hill (1965) and Budiansky (1965).

It can be declared that one of the first classic self-consistent analyses in the field of effective medium methods was introduced by Sabina and Willis (1988), which also provides appropriate results in high volume fractions. In this method, the phase velocity and attenuation of the coherent wave is obtained in an iterative process. Sabina and Willis demonstrated that the obtained self-consistency generate acceptable answers to determine effective dynamic properties just when wavelength of the elastic waves is at least four times that of radius of spherical inclusions.

Kim et al. (1995) presented an estimation of the effective dynamic properties and effective density which is similar to the coherent potential approximation in alloy physics. The obtained theoretical results are closer to the Kinra's experimental results as compared to Ying & Truell (1956) results. Both of these methods show elastic properties similar to the static analysis results of Hill and Budiansky.

There are various micromechanical methods for estimation of static elastic moduli of the composites, for example self-consistent, generalized self-consistent and Mori-Tanaka methods. Although all these techniques provide acceptable results at low volume fractions, Christensen (1990) demonstrated that only the generalized self-consistent method is able to give acceptable results at great volume fractions. Yang (2003) developed this model for studying multiple scattering of the plane longitudinal and shear waves in particulate composites of random distribution. He also showed that this model offers better results in dense composites in comparison with the effective field methods.

Kanaun and his colleagues (2004, 2005, 2007) extracted scattering equations of longitudinal and shear elastic waves in composite materials containing spherical particles that are distributed randomly. They showed that each of these methods has some advantages over the others.

Different works have been done in the field of experimental evaluation of plane elastic wave propagation in particulate composites. Kinra et al. (1982, 1997) experimentally studied propagation of ultrasonic elastic waves in composites containing spherical particles which are distributed randomly in the matrix medium. Layman et al. (2006) measured phase velocity and attenuation of the longitudinal and shear waves in these composites. By comparing the results obtained with two theoretical models of Waterman-Truell and generalized self-consistent they showed that both models perform almost similarly, though the generalized self-consistent model is more accurate in higher volume fractions.

The main objective here is to examine propagation of the longitudinal elastic waves in the particulate composites which contain stiff, soft, light and heavy spherical inclusions in addition to compare different approaches in this regard. For this purpose, four methods namely Foldy, Waterman-Truell, generalized self-consistent and Sabina-Willis were compared with each other for solving the problem.

2 WAVE PROPAGATION THROUGH AN INFINITE MEDIUM WITH SPHERICAL HETEROGENEITY

When a pressure wave impinges on the elastic surface of heterogeneity, two longitudinal and shear waves are reflected from the surface outward the heterogeneity, while two other waves will be propagated inside the heterogeneity. Figure 1 depicts schematic of this problem. In equation (1), it can be seen that the physical and mechanical specifications of the matrix medium are denoted by subscript 2, while the spherical heterogeneity is labeled with subscript 1. Moreover, the functions of potential, displacements and stresses related to incident wave, reflected wave and the wave refracted into the heterogeneity are shown with superscripts (i), $(r)$and (f), respectively.

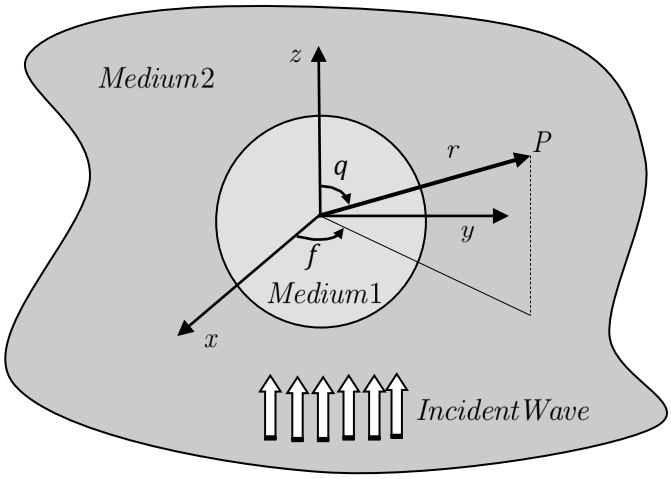

Figure 1 schematic illustration of P wave diffraction by a spherical inclusion.

Equation of the incident plane longitudinal wave which propagates in the positive z-direction is as below:

$$\varphi^{(i)} = \varphi_0 e^{i\left(k_2 z - \omega t\right)} = \varphi_0 \, e^{-i\omega t} \sum_{n=0}^{\infty} \left(2n+1\right) i^n \, j_n\left(k_2 r\right) P_n\left(cos\theta\right) \tag{1}$$

Where, k_2 represents the longitudinal wave number in the matrix medium and ω denotes circular frequency of the incident wave. When the plane elastic wave propagates toward the z-direction, the potential and displacement functions will be independent of ϕ in spherical coordinates. The potential functions are given below for the two waves reflected outward the heterogeneity:

$$\varphi^{(r)} = \sum_{n=0}^{\infty} A_n \, h_n^{(1)}\left(k_2 r\right) P_n\left(cos\theta\right) e^{-i\omega t} \tag{2}$$

$$\chi^{(r)} = \sum_{n=0}^{\infty} B_n h_n^{(1)}\left(K_2 r\right) P_n\left(cos\theta\right) e^{-i\omega t} \tag{3}$$

And for two waves refracted toward inside the heterogeneity:

$$\varphi^{(f)} = \sum_{n=0}^{\infty} C_n j_n\left(k_1 r\right) P_n\left(cos\theta\right) e^{-i\omega t} \tag{4}$$

$$\chi^{(f)} = \sum_{n=0}^{\infty} D_n j_n\left(K_1 r\right) P_n\left(cos\theta\right) e^{-i\omega t} \tag{5}$$

In the abovementioned equations, k_1, k_2, K_1, K_2 are the longitudinal and shear wave numbers of 1 and 2 media. The unknown coefficients of A_n, B_n, C_n, D_n are also determined by considering boundary conditions. The boundary conditions in the matrix and heterogeneity interface (i.e. $r = a$) are continuity of stresses and displacements which is given as below:

$$u_r^{(i)} + u_r^{(r)} = u_r^{(f)} \tag{6}$$

$$u_q^{(i)} + u_q^{(r)} = u_q^{(f)} \tag{7}$$

$$\sigma_{rr}^{(i)} + \sigma_{rr}^{(r)} = \sigma_{rr}^{(f)} \tag{8}$$

$$\sigma_{r\theta}^{(i)} + \sigma_{r\theta}^{(r)} = \sigma_{r\theta}^{(f)} \tag{9}$$

In the matrix medium, the equations of displacements and stresses are stated as below due to propagation of the incident wave in addition to the waves reflected from surface of the heterogeneity as follows:

$$u_{r2} = \frac{1}{r}\sum_{n=0}^{\infty}\left(\varphi_0 Q_{71}^{(1)} + A_n Q_{71}^{(3)} + B_n Q_{72}^{(3)}\right) P_n\left(cos\theta\right) \tag{10}$$

$$u_{\theta 2} = \frac{1}{r}\sum_{n=0}^{\infty}\left(\varphi_0 Q_{81}^{(1)} + A_n Q_{81}^{(3)} + B_n Q_{82}^{(3)}\right) \frac{dP_n\left(cos\theta\right)}{d\theta} \tag{11}$$

$$\sigma_{rr2} = \frac{2\mu_2}{r^2}\sum_{n=0}^{\infty}\left(\varphi_0 Q_{11}^{(1)} + A_n Q_{11}^{(3)} + B_n Q_{12}^{(3)}\right) P_n\left(cos\theta\right) \tag{12}$$

$$\sigma_{r\theta 2} = \frac{2\mu_2}{r^2}\sum_{n=0}^{\infty}\left(\varphi_0 Q_{41}^{(1)} + A_n Q_{41}^{(3)} + B_n Q_{42}^{(3)}\right) \frac{dP_n\left(cos\theta\right)}{d\theta} \tag{13}$$

Similarly, for the medium 1, displacements and stresses equations due to propagation of the waves refracted into the sphere are listed as below:

$$u_{r1} = \frac{1}{r}\sum_{n=0}^{\infty}\left(C_n W_{71}^{(1)} + D_n W_{72}^{(1)}\right)P_n\left(cos\theta\right) \tag{14}$$

$$u_{\theta 1} = \frac{1}{r}\sum_{n=0}^{\infty}\left(C_n W_{81}^{(1)} + D_n W_{82}^{(1)}\right)\frac{dP_n\left(cos\theta\right)}{d\theta} \tag{15}$$

$$\sigma_{rr1} = \frac{2\mu_1}{r^2}\sum_{n=0}^{\infty}\left(C_n W_{11}^{(1)} + D_n W_{12}^{(1)}\right)P_n\left(cos\theta\right) \tag{16}$$

$$\sigma_{r\theta 1} = \frac{2\mu_1}{r^2}\sum_{n=0}^{\infty}\left(C_n W_{41}^{(1)} + D_n W_{42}^{(1)}\right)\frac{dP_n\left(cos\theta\right)}{d\theta} \tag{17}$$

The relations between internal terms of the abovementioned equations are listed in Appendix 1.

3 SELF-CONSISTENT METHODS IN MULTIPLE SCATTERING OF WAVES IN MULTIPHASE MEDIA

Since it is impossible to accurately solve the problems related to multiple scattering in random media, approximate methods are expected to be the main approach for solving these problems. The methods are based on simple hypotheses which reduce the problem of multiple scattering and mutual effects between heterogeneities to a simple scattering problem of single heterogeneity. This approach can be divided into two main categories, namely effective field methods and effective medium methods.

3.1 Methods of Effective Field

This set of methods is based on the following hypotheses (Kanaun et al. 2005):

- Each particle acts as a single particle inside the primary matrix,
- The effect of other surrounding particles is considered as an effective field which is applied on that particle.

The second hypothesis is the base of different works in this field. The simplest approach in this regard is that the effective field is considered as a plane wave which is identical for all the particles. This approximation is usually known as quasi-crystalline estimation. The models developed by Foldy and Waterman-Truell are among the most famous methods of the effective field.

3.2 Methods of Effective Medium

Effective medium methods are based on two following assumptions (Kanaun et al. 2004):

- Each particle in a heterogeneous medium acts as a single particle inside a homogeneous medium, such that this homogeneous medium will get the effective properties of the heterogeneous medium.
- Average wave field is matched with the wave field propagated inside the homogeneous medium (self-consistency condition).

In this kind of methods, there are also some additional editions for the first hypothesis of the problem. For instance, behavior of each particle in the heterogeneous medium is modeled as a single particle with a layer of matrix which is embedded in the effective homogeneous medium. The models of Sabina-Willis and generalized self-consistent are some of these methods.

4 FORMULATION

4.1 Foldy's Model

The first work based on the compatible wave treatments in the field of multiple scattering of scalar waves in media containing elastic and isotropic scatterers with random distribution was directed by Foldy. He demonstrated that the average wave field in a medium which contain randomly distributed scatterers satisfies the wave equation in a continuous medium without scatterers. However, the propagation constant of this equivalent medium differs. The complex propagation constant finally proposed by Foldy for a medium with n_0 scatterers per unit volume as below:

$$\left\langle k\right\rangle^2 = k_2^2 + 4\pi n_0 f\left(0\right) \tag{18}$$

$$\left\langle K\right\rangle^2 = K_2^2 + 4\pi n_0 g\left(0\right) \tag{19}$$

Where, k_2 and K_2 represent propagation constants of P and S waves, while $f\left(0\right)$ and $g\left(0\right)$ denote forward far field scattering amplitude of longitudinal and shear waves, respectively.

4.2 Waterman-Truell Model (WT)

Waterman & Truell introduced an approach in 1961 for calculation of the total effective field and properties of wave propagation in a medium containing randomly distributed scatterers. They expressed these parameters versus the number of scatterers per unit volume along with the forward and backward longitudinal and shear scattered wave amplitude by a single inclusion. They developed a statistical averaging process in order to estimate the wave propagation constant. In fact, they found properties of an equivalent homogeneous medium which has an effective complex wave number by using physical and mechanical properties of the original heterogeneous medium. The following equations are proposed for longitudinal and shear waves by the model, respectively:

$$\left[\frac{\left\langle k\right\rangle}{k_2}\right]^2 = \left[1 + \frac{2\pi n_0 f\left(0\right)}{k_2^2}\right] - \left[\frac{2\pi n_0 f\left(\pi\right)}{k_2^2}\right] \tag{20}$$

$$\left[\frac{\langle K\rangle}{K_2}\right]^2=\left[1+\frac{2\pi n_0 g(0)}{K_2^2}\right]-\left[\frac{2\pi n_0 g(\pi)}{K_2^2}\right] \tag{21}$$

Where, a is radius of the identical scatteres. Equations 20 and 21 are also used for the longitudinal and shear waves, respectively.

The Waterman-Truell model ignores the correlation between the inclusions, so this model can be used only if density of the scatterers is small in the matrix medium. Therefore, this theory would be unable to describe accurately the problem of dens mediums.

4.3 Dynamic Generalized Self-consistent Model (DGSCM)

Yang (2003) proposed his dynamic generalized self-consistent model for the two-phase composites considering longitudinal and shear propagated waves in the presence of cylindrical and spherical inclusions. Figure 2 illustrates the intrinsic geometry that this model is based on. A random distribution of the identical spherical inclusions with radius a embedded in an infinite isotropic matrix was considered for explanation of the model. Moreover, it was assumed that λ_1, μ_1 and ρ_1 are Lame constants and mass density of the scatterers, while λ_2, μ_2 and ρ_2 are those of the matrix.

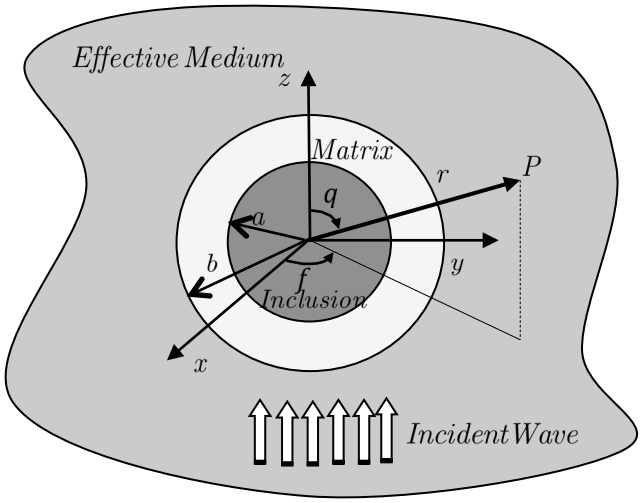

Figure 2 Sketch of dynamic generalized self-consistent model.

In the schematic view displayed, (x,y,z) shows the Cartesian coordinate system and (r,θ,ϕ) represents the polar Spherical coordinate system. Meanwhile, components of the displacement vector in r and θ directions are denoted by u_r and u_q respectively. The governing equation in the problem can be given as below:

$$\left(\lambda+2\mu\right)\nabla\nabla.\mathbf{u}-\mu\nabla\times\nabla\times\mathbf{u}=\rho\frac{\partial^2\mathbf{u}}{\partial t^2} \tag{22}$$

In this model, the spherical scatterer with radius a is embedded in a spherical shell of the matrix with outer radius b. An infinite medium with the effective Lame constants of $\langle\lambda\rangle$ and $\langle\mu\rangle$, and the effective mass density of $\langle\rho\rangle$ includes this system. The relation between assumed radius of b and particles volume concentration called c is given below:

$$c=\frac{a^3}{b^3} \tag{23}$$

In the composite materials with a small difference between constituents density, one may use the mean density instead of the effective density as below:

$$\langle\rho\rangle=c\rho_1+\left(1-c\right)\rho_2 \tag{24}$$

However, for the composite materials with high density contrast, the effective density will depend on the frequency of incident wave. In this case, the equation of effective density proposed by Sabina & Willis can be utilized.

When the incident wave is a plane longitudinal one, components of the displacement vectors and the stress tensor can be expressed as u_r, u_q and s_{rr}, s_{rq} respectively. Furthermore, the stress components can be found from the related displacement components through the stress-displacement relations:

$$\frac{\sigma_{rr}}{\mu}=\frac{\lambda}{\mu}\frac{1}{r^2sin\theta}\left[\frac{\partial}{\partial r}\left(r^2u_r sin\theta\right)+\frac{\partial}{\partial\theta}\left(ru_\theta sin\theta\right)+\frac{\partial}{\partial\phi}\left(ru_\phi\right)\right]+2\frac{\partial u_r}{\partial r} \tag{25}$$

$$\frac{\sigma_{r\theta}}{\mu}=\frac{1}{r}\frac{\partial u_r}{\partial\theta}+\frac{\partial u_\theta}{\partial r}-\frac{u_\theta}{r} \tag{26}$$

Assuming a perfect bonding between the constituents and the matrix, the boundary conditions can be stated as the continuity of displacement and stress at the interfaces:

$$u_{r2}\left(r,\theta\right)\Big|_{r=a}=u_{r1}\left(r,\theta\right)\Big|_{r=a} \tag{27}$$

$$u_{\theta2}\left(r,\theta\right)\Big|_{r=a}=u_{\theta1}\left(r,\theta\right)\Big|_{r=a} \tag{28}$$

$$u_{re}\left(r,\theta\right)\Big|_{r=b}=u_{r2}\left(r,\theta\right)\Big|_{r=b} \tag{29}$$

$$u_{\theta e}(r,\theta)\Big|_{r=b} = u_{\theta 2}(r,\theta)\Big|_{r=b} \tag{30}$$

$$\sigma_{rr2}(r,\theta)\Big|_{r=a} = \sigma_{rr1}(r,\theta)\Big|_{r=a} \tag{31}$$

$$\sigma_{r\theta 2}(r,\theta)\Big|_{r=a} = \sigma_{r\theta 1}(r,\theta)\Big|_{r=a} \tag{32}$$

$$\sigma_{rre}(r,\theta)\Big|_{r=b} = \sigma_{rr2}(r,\theta)\Big|_{r=b} \tag{33}$$

$$\sigma_{r\theta e}(r,\theta)\Big|_{r=b} = \sigma_{r\theta 2}(r,\theta)\Big|_{r=b} \tag{34}$$

Substituting the total displacement field of the effective medium, matrix and inclusion in the boundary conditions, the following matrix equation is obtained for the case of plane longitudinal incident wave:

$$\begin{bmatrix} \mathbf{P} & -\mathbf{P}^{(2)} & -\tilde{\mathbf{P}}^{(2)} & 0 \\ \alpha\mathbf{Q} & -\mathbf{Q}^{(2)} & -\tilde{\mathbf{Q}}^{(2)} & 0 \\ 0 & \mathbf{P}^{(1)} & \tilde{\mathbf{P}}^{(1)} & -\mathbf{P}^{0} \\ 0 & \mathbf{Q}^{(1)} & \tilde{\mathbf{Q}}^{(1)} & \beta\mathbf{Q}^{0} \end{bmatrix} \begin{Bmatrix} A_{mn} \\ C_{mn} \\ A'_{mn} \\ C'_{mn} \\ D_{mn} \\ F_{mn} \\ A^{0}_{mn} \\ C^{0}_{mn} \end{Bmatrix} = -\begin{bmatrix} \tilde{\mathbf{P}} \\ \alpha\tilde{\mathbf{Q}} \\ 0 \\ 0 \end{bmatrix} \begin{Bmatrix} \Phi_{mn} \\ X_{mn} \end{Bmatrix} \tag{35}$$

By solving the abovementioned set of equations, the unknown coefficients can be found. Detailed descriptions of the parameters are stated in Appendix 2. The basic equations for defining propagation constants of the average wave in the effective medium can be stated as below:

$$\left[\frac{k^{(j+1)}}{k^{(j)}}\right]^2 = \left[1 + \frac{2\pi n_0 f^{(j)}(0)}{\left[k^{(j)}\right]^2}\right]^2 - \left[\frac{2\pi n_0 f^{(j)}(\pi)}{\left[k^{(j)}\right]^2}\right]^2 \tag{36}$$

$$\left[\frac{K^{(j+1)}}{K^{(j)}}\right]^2 = \left[1 + \frac{2\pi n_0 g^{(j)}(0)}{\left[K^{(j)}\right]^2}\right]^2 - \left[\frac{2\pi n_0 g^{(j)}(\pi)}{\left[K^{(j)}\right]^2}\right]^2 \tag{37}$$

In which, the forward and backward scattering amplitudes for the case of longitudinal incident wave is given as below:

$$f^{(j)}(0)=\sum_{n=0}^{\infty}(-i)^n A_{0n}^{(j)} \tag{38}$$

$$f^{(j)}(\pi)=\sum_{n=0}^{\infty}(i)^n A_{0n}^{(j)} \tag{39}$$

$$g^{(j)}(0)=\sum_{n=1}^{\infty}\frac{(-i)^n}{2}\left[n(n+1)C_{1n}^{(j)}+C_{-1n}^{(j)}\right] \tag{40}$$

$$g^{(j)}(\pi)=\sum_{n=1}^{\infty}\frac{(i)^n}{2}\left[n(n+1)C_{1n}^{(j)}+C_{-1n}^{(j)}\right] \tag{41}$$

These equations are solved in an iterative process to yield the required convergence. Meanwhile, the initial values are taken equal to those properties of the matrix material.

4.4 Sabina-Willis Model (SW)

Sabina & Willis tried to offer a simple self-consistent solution for dealing with the problem of wave propagation in heterogeneous media. This model considers a heterogeneous material which is comprised of a matrix and random distribution of n types embedded inclusions. The matrix has density of r_{n+1} and a tensor of elastic moduli L_{n+1}, and each inclusion of type r having density r_r and tensor of elastic moduli L_r, respectively, such that $r=1,2,\ldots,n$. In addition, all inclusions of type r have the same size and shape.

In a specific loading, the displacement field u in the medium depends on the exact configuration of the heterogeneities. Thus, determination of the average displacement field $\langle u\rangle$ will be considered instead of the exact displacement field because of the random distribution of the inclusions. Response of the composite to any kind of loading obeys the equation of motion. In the absence of the body forces the equation of motion is:

$$\nabla\bullet\sigma=\dot{p} \tag{42}$$

Where, stress σ and momentum density p are related to strain e and velocity as:

$$\sigma=Le \tag{43}$$

$$p=\rho\dot{u} \tag{44}$$

Where, $\dot{u}$ is the velocity and ρ stands for the mass density. The tensor of elastic moduli L and the mass density ρ are extracted as below versus position x as:

$$L(x)=\sum_{r=1}^{n+1}L_r f_r(x) \tag{45}$$

$$\rho(x)=\sum_{r=1}^{n+1}\rho_r f_r(x) \tag{46}$$

Where:

$$f_r(x)=\begin{cases} 1; x\in \textit{material } r \\ 0; \quad \textit{otherwise} \end{cases} \tag{47}$$

By averaging from the equation above and following the analysis of Hill in the static analysis, it is found that:

$$\langle\sigma\rangle=L_{n+1}\langle e\rangle+\sum_{r=1}^{n}c_r\left(L_r-L_{n+1}\right)\langle e\rangle_r \tag{48}$$

$$\langle p\rangle=\rho_{n+1}\langle\dot{u}\rangle+\sum_{r=1}^{n}c_r\left(\rho_r-\rho_{n+1}\right)\langle\dot{u}\rangle_r \tag{49}$$

Where, c_r is the probability density function for the particles of type r. Therefore, the desired effective equations can be obtained if one could represent $\langle e\rangle_r$ and $\langle\dot{u}\rangle_r$ in terms of $\langle e\rangle$ and $\langle\dot{u}\rangle$. One simple approach to deal with this problem is to consider a single inclusion embedded in a homogeneous medium with the effective properties of the composite material. By using the two fundamental assumptions in the effective medium methods and based on the abovementioned equations, the effective elastic properties of a multiphase composite can be derived from the following equations:

$$L_{eff}=L_{n+1}+\sum_{r=1}^{n+1}c_r h_r(q)h_r(-q)\left(L_r-L_{n+1}\right)\left[I+S_x^r\left(L_r-L_{eff}\right)\right]^{-1} \tag{50}$$

$$\rho_{eff}=\rho_{n+1}+\sum_{r=1}^{n+1}c_r h_r(q)h_r(-q)\left(\rho_r-\rho_{n+1}\right)\left[I+M_x^r\left(\rho_r-\rho_{eff}\right)\right]^{-1} \tag{51}$$

The effective dynamic properties which are extracted from this model can be summarized as follows for a two-phase medium containing a random distribution of the spherical particles:

$$B = B_2 + \frac{ch(q)h(-q)(B_1 - B_2)}{1+3(B_1 - B)\varepsilon_p / (3B+4\mu)} \tag{52}$$

$$\mu = \mu_2 + \frac{ch(q)h(-q)(\mu_1 - \mu_2)}{1+2(\mu_1 - \mu)\left[2\mu\varepsilon_p + (3B+4\mu)\varepsilon_s\right] / \left[5\mu(3B+4\mu)\right]} \tag{53}$$

$$\rho = \rho_2 + \frac{ch(q)h(-q)(\rho_1 - \rho_2)}{1+(\rho_1 - \rho)(3 - \varepsilon_p - 2\varepsilon_s) / (3\rho)} \tag{54}$$

Where the function $h(q)$ for the spherical inclusions is given as below:

$$h(q) = 3\left[sin(qa) - qacos(qa)\right] / (qa)^3 \tag{55}$$

In which the wave number of q is substituted with k and K in the longitudinal and shear incident wave, respectively. Moreover, the terms ε_p and ε_s are stated as below:

$$\varepsilon_p = 3(1 - ika)\left[sin(ka) - kacos(ka)\right]\left(e^{ika}\right) / (ka)^3 \tag{56}$$

$$\varepsilon_s = 3(1 - iKa)\left[sin(Ka) - Kacos(Ka)\right]\left(e^{iKa}\right) / (Ka)^3 \tag{57}$$

5 NUMERICAL ANALYSIS

As we know in the wave propagation study, the scattering phenomenon may be caused by two factors, namely variation in the mass density or the elastic properties of the constituent phases. Thus, to illustrate the nature and general behavior of the composites, the constituents are chosen such that the effect of variations in mass density and elastic properties on the average wave field can be evaluated. So in the first set of considered composites, the mass density was taken the same for both phases, and the elastic constants of inclusions were taken first twice and another time half of the elastic constants of the matrix in two different cases. In the second set of assumed composites, the elastic constants of the both phases were taken the same, while the mass density was assumed to be twice and half of the mass density of the matrix medium. Properties of the considered composite constituents are listed in Table 1.

Table 1 Mechanical properties of constituents. ($r_2 = 2.7\ (\mathrm{g/cm^3})$, $B_2 = 75.2\ (\mathrm{GPa})$, $m_2 = 34.7\ (\mathrm{Gpa})$)

	Shear Modulus (GPa)	Bulk Modulus (GPa)	Density ($\mathrm{g/cm^3}$)
Matrix	μ_2	B_2	ρ_2
Soft Inclusion	$\mu_2/2$	$B_2/2$	ρ_2
Stiff Inclusion	$2\mu_2$	$2B_2$	ρ_2
Heavy Inclusion (HD)	μ_2	B_2	$2\rho_2$
Light Inclusion (LD)	μ_2	B_2	$\rho_2/2$

It is appropriate to divide the elastic wave propagation investigation into three categories according to the inclusion size and the incident wavelength. A dimensionless parameter of $\delta = \lambda/a$ is defined first which is indicative of the incident wavelength to radius of the spherical inclusion. Based on this definition, the dimensionless wave number is given as $k_2 a = 2\pi/\delta$. Three different frequency ranges can be studied. If wavelength of the incident wave is much larger than radius of the spherical heterogeneities ($\delta >> 1$), then the incident wave will be located within the range of long wavelength or low frequency regime. Meanwhile, if the incident wavelength is close to size of the heterogeneities ($\delta \approx 1$), then it is located within the range of intermediate wavelength or frequency. In the last case, if this ratio is significantly small ($\delta << 1$), then the incident wave will be within the range of short wavelengths or high frequency regime. The desired range here in this study includes long to intermediate wavelengths which will be discussed in this section.

Figure 3 depicts the variations in normalized phase velocity and attenuation of the longitudinal average wave in terms of dimensionless wave number and volume fraction of soft, stiff, light and heavy inclusions using the dynamic generalized self-consistent model.

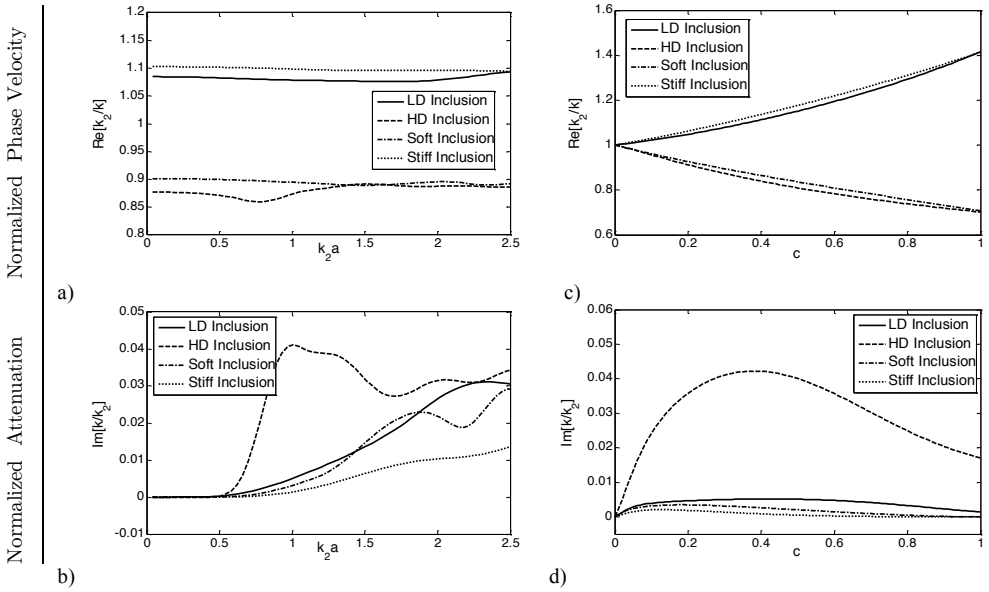

Figure 3 Variation of normalized phase velocity and attenuation of P wave with the normalized frequency ($c = 0.3$) and volume concentration ($k_2 a = 1$) using DGSCM.

As can be seen in Figure 3a, the normalized phase velocity in all cases is first decreased at low frequencies and then increased a bit. As long as frequency of the incident wave is located within range of low frequency or long wavelength, variations of the phase velocity versus the frequency can be ignored. Indeed, the composite material demonstrates a static behavior in a long wavelength regime. This can be attributed to the small scattering in the long wavelength. When frequency of the incident wave approaches to intermediate frequency or wavelength range, curve of the phase velocity will get an ascending trend. Therefore, greater variations can be seen in the phase velocity of the composite versus frequency. Moreover, the phase velocity of the average wave will be greater in composites containing stiff or light particles and will be smaller in composites containing soft or heavy particles in comparison with those of the matrix. This is because effective wave number is conversely related to squared elastic constants of the effective medium and directly related to squared mass density of the effective medium.

Figure 3b illustrates the normalized attenuation versus dimensionless wave number. Variation in attenuation of the coherent wave is discussed in the composite material which contains soft inclusions. The curve starts from zero point and takes an ascending trend by increasing the wave frequency. It can be observed that the curve has numerous maximum and minimum points which can be assigned to resonance frequencies of the spherical inclusion. Kinra has showed that the wave propagation behavior in particulate composites is noticeably affected by resonances of the particles. It should be noted that the lowest resonance mode which can be inferred as the rigid-body oscillation cannot be seen in the composites containing considered soft and stiff particles because this mode appears when the difference between mass density of the heterogeneities and the matrix is significant. If not, the difference in the inertia force between the matrix and inclusions will be small and thus unable to excite the rigid-body resonance mode. As a result, the maximum and minimum points seen in the diagram are related to the resonances of higher modes, which are the elastic resonance modes. This can be justified by the difference in stiffness of the two media.

But in the presence of considered light or heavy particles, the first maximum point in the attenuation curve belongs to rigid-body oscillation of the spherical particle embedded in the medium according to strong contrast of mass densities. This resonance frequency creates a maximum point in the attenuation curve and initiates rise in the curve of phase velocity. These simultaneously changes can be explained by Kramers-Kronig relation. The dominant mechanism for attenuation of coherent wave in particulate composites is scattering into incoherent waves. And it can be occurred outside the low frequency range where $\delta \approx 1$ or $\delta << 1$. So, as can be seen from the figure, attenuation of all composite materials in $k_2 a \le 0.5$ is very small and even negligible in the range of low frequency. Meanwhile, the attenuation in the composite materials containing heavy particles is greater than the case of light particles, while this amplitude for soft particles is greater than that of stiff particles. This observation can be explained by this fact that due to small velocity of the elastic waves in soft or heavy materials, a greater contribution of the incident wave is scattered outward so that the amplitude of final wave will be much smaller.

Figure 3c illustrates variation of the phase velocity for the average wave versus particles volume fraction. As evident from the curve, it is decreased by increasing the particles volume fraction in the presence of soft ones. This is because density remains unchanged by raising the volume fraction of soft particles but final stiffness of the composite material is reduced. In this case, the wave propaga-

tion speed through the effective medium is decreased as compared to that of the matrix. An ascending trend will be seen in the curve of phase velocity with the same explanation if stiff particles exist. Thereby, the normalized phase velocity curve will be ascending and descending in the presence of light and heavy particles, respectively. All the curves of phase velocity begin from 1 in $c=0$ which can be justified with respect to normalizing of the phase velocity against those of the matrix medium.

Figure 3d presents variation of the attenuation versus volume fraction of the constituent particles. It can be observed that the attenuation curve increases by raising the volume fraction of the particles, and then decreases again after reaching a maximum point. When the volume fraction of the particles is $c=0$ or $c=1$, the attenuation is expected to be zero due to creating a homogeneous medium. This constraint is satisfied about the soft and stiff particles in which the mean density equation is utilized, but this constraint is not met at $c=1$ for light and heavy particles. Furthermore, since the maximum spatial fluctuation in properties of the composites occurs in $c=0.5$, it is expected that a maximum point will exists somewhere near this value. The investigation was done for the frequency of $k_2a=1$. The ratio of incident wave to radius of the spherical particles will be $\delta=2\pi$ in this case which is located within the range of the intermediate wavelength. In the composite with soft particles, the maximum attenuation is created at $c=0.16$ for $k_2a=1$. Meanwhile, as clearly evident, the attenuation in all volume fractions for the composites with heavy particles will be greater than those containing the light ones. The same regime is seen for soft and stiff particles, in which the attenuation amplitude of the former is greater than that of the latter.

Figure 4a shows variations of the shear modulus versus the dimensionless wave number for the considered composites. Trend of changes in the shear modulus of the effective medium in this figure in state of soft and stiff particles is similar with the trend explained in the curve of normalized phase velocity versus dimensionless wave number. It is expected that the normal shear modulus of the effective medium in the presence of stiff particles is greater than unit, while this value is predicted to be smaller than unit in the presence of soft particles. Regarding the composites with light and heavy particles, the effective shear modulus is expected not to change with the dimensionless wave number since the constituents elastic properties are the same. However, this is only seen at low frequency regime.

Figure 4b shows variation of the shear modulus of effective medium versus volume fraction. One interesting point in all curves obtained from this model is that if the soft and stiff particles are increased, then the elastic properties of the effective medium will become smaller and greater than those of the matrix, respectively. In the case of soft and stiff particles at $c=1$, the effective shear modulus become half and twice that of the matrix medium, respectively. This is in agreement with the initial assumption of elastic properties for the components. Nevertheless, the expectation for remaining the elastic properties unchanged by increasing the volume fraction of light and heavy particles is not met completely in this model and there are still some small variations in versus the volume concentration. A similar behavior is obtained in the curves of Figures 4c and 4d for bulk modulus of the effective medium.

Variation of the normalized mass density of the effective medium as a function of the wave number are demonstrated in Figure 4e The effective mass density is constant and equal to unit for soft and stiff particles. However, about light and heavy particles, dominant behavior of the curve is

mainly ascending and descending, respectively. The effective density in both cases experiences just small variations in the range of low frequency and small volume fractions.

Figure 4f shows the parameter in terms of volume concentration. It can be seen that increasing the volume fraction does not show any variation in the effective density of composite materials which contain soft and stiff particles. Moreover, prediction of an ascending and descending trend is consistent with the physical expectation of the problem for the presence of heavy and light particles, respectively. However, predicting the final mass density of the effective medium at $c=1$ is not the same as the expected values accurately such that $Re[\rho/\rho_2]=0.43$ and $Re[\rho/\rho_2]=1.67$ are found for the light and heavy particles, respectively.

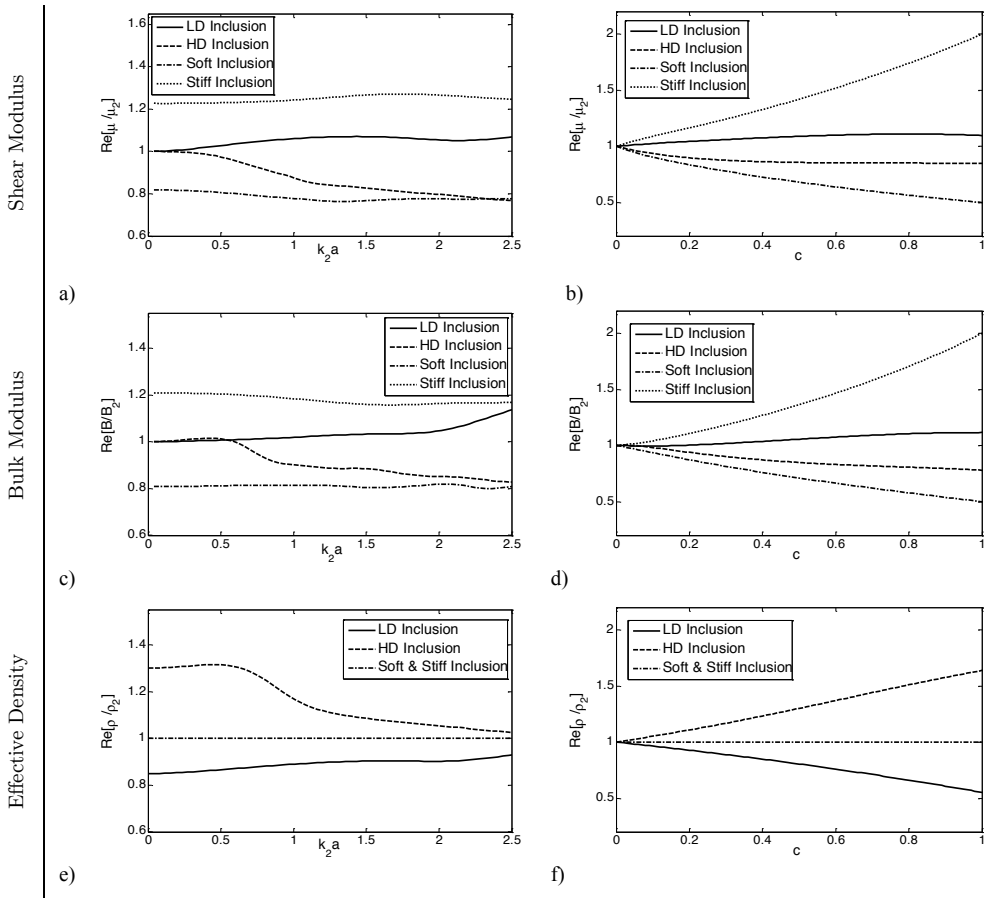

Figure 4 Variation of the effective elastic constants and effective density with the normalized frequency ($c=0.3$) and volume concentration ($k_2a=1$) using DGSCM.

Figure 5 displays the numerical results of the normalized phase velocity and attenuation versus the dimensionless wave number at $c=0.15$. The results obtained with four models of Foldy, WT, SW and DGSCM are drawn next to each other for the purpose of comparison. Some interesting points can be made from these diagrams which will come in the following: All the models display a mutation rapid rise in the range of low frequency for the composites with heavy particles. This behavior which is seen in most of the composite with heavy particles is due to the rigid-body reso-

nance of particles which was mentioned before. Although all the models demonstrate this phenomenon properly, the DGSCM model predicts a much greater frequency of resonance.

Meanwhile, as can be seen in attenuation curves of the other composites, the effective field models of WT and Foldy predict greater attenuation amplitude as compared to that of the effective medium methods of SW and DGSCM. Moreover, it can be concluded from comparing the four abovementioned models in all the attenuation curves that the models of SW, Foldy and WT predict similar values but different to the DGSCM model. About the SW model, it must be noted that the results are acceptable up to the frequency range of $k_2 a = \pi/2$. As previously mentioned, the maximum propagated wavelength can be at least four times greater than radius of the reinforcement spherical particles. By looking at the curves of normalized phase velocity in this figure it can also be inferred that the effective medium methods of SW and DGSCM have assigned the boundary ranges of maximum and minimum values respectively, depending on type of the composite material except for the low frequency ranges.

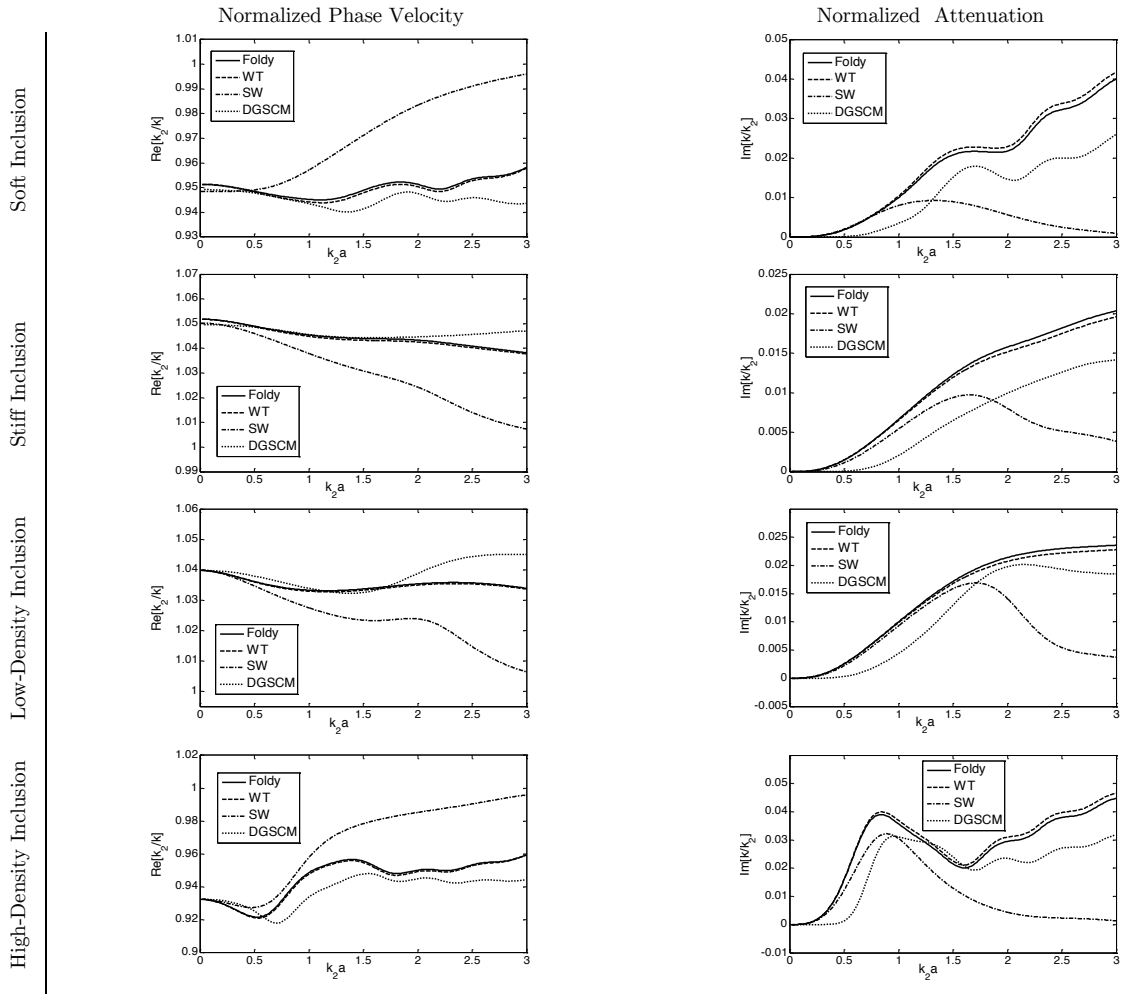

Figure 5 Normalized phase velocity and attenuation of P wave versus dimensionless frequency predicted by different models for $c = 0.15$.

Figure 6 depicts results of the normalized phase velocity and attenuation versus volume fraction at $k_2a=1$. In this frequency, the wavelength is about 6.28 times greater than radius of the spherical particles which indicates location in the range of the intermediate wavelength. Since the greatest distinction between properties of the heterogeneous medium occurs at $c=0.5$, from the microstructural point of view, a maximum point is expected to be seen in the attenuation curve. Comparison of the models in this figure implies that the SW and DGSCM techniques have successfully attained a good estimation in this regard. But, the effective field methods are unable to predict the existence of this maximum point.

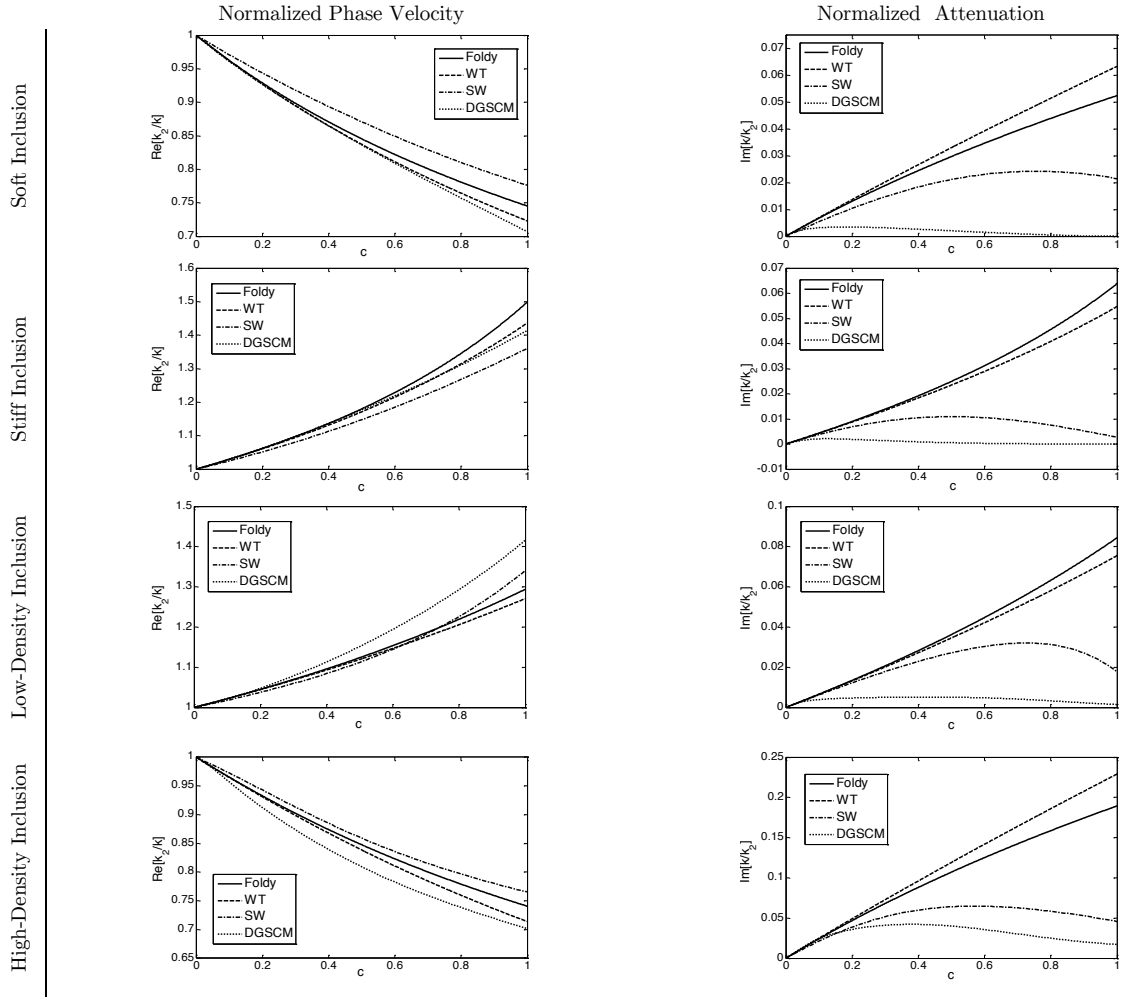

Figure 6 Normalized phase velocity and attenuation of P wave versus volume concentration predicted by different models for $k_2a=1$.

Attenuation of the coherent wave at the boundaries are other points under study which can be considered. Considering the homogenization of the medium and having no macroscopic randomness at $c=0$ and $c=1$, zero attenuation is expected for all cases. All models satisfy this condition at $c=0$. This condition is still satisfied at $c=1$ in the DGSCM model for the composites with soft and stiff particles where the equation of mean density is utilized. However, for the composites which

contain light and heavy particles, this model approximately predicts zero wave attenuation. Moreover, all the models in the range of low frequency predict almost the same values. Studying the normalized phase velocity versus volume fraction, it is properly evident that the DGSCM model proposed more accurate values at the boundaries in comparison with the other models, while all the models can perform successfully in addressing the ascending and descending trend of the phase velocity versus volume fraction.

Figure 7 indicates variations of the shear and bulk modulus of the effective medium based on the effective medium models of SW and DGSCM in terms of the dimensionless wave number at $c = 0.15$. As shown by the figure, both models provide a good consistency in prediction of the bulk modulus of the effective medium in low and intermediate frequency regime. The SW model properly predicts constants values of the effective dynamic properties at different frequencies in the composites which contain light and heavy particles. However, the model of DGSCM shows small variations for the composites with light particles and greater variations for those containing heavy particles in terms of frequency. Furthermore, the difference between these two models in prediction of the effective dynamic values of the composites containing soft and heavy particles is more significant than those with stiff and light particles.

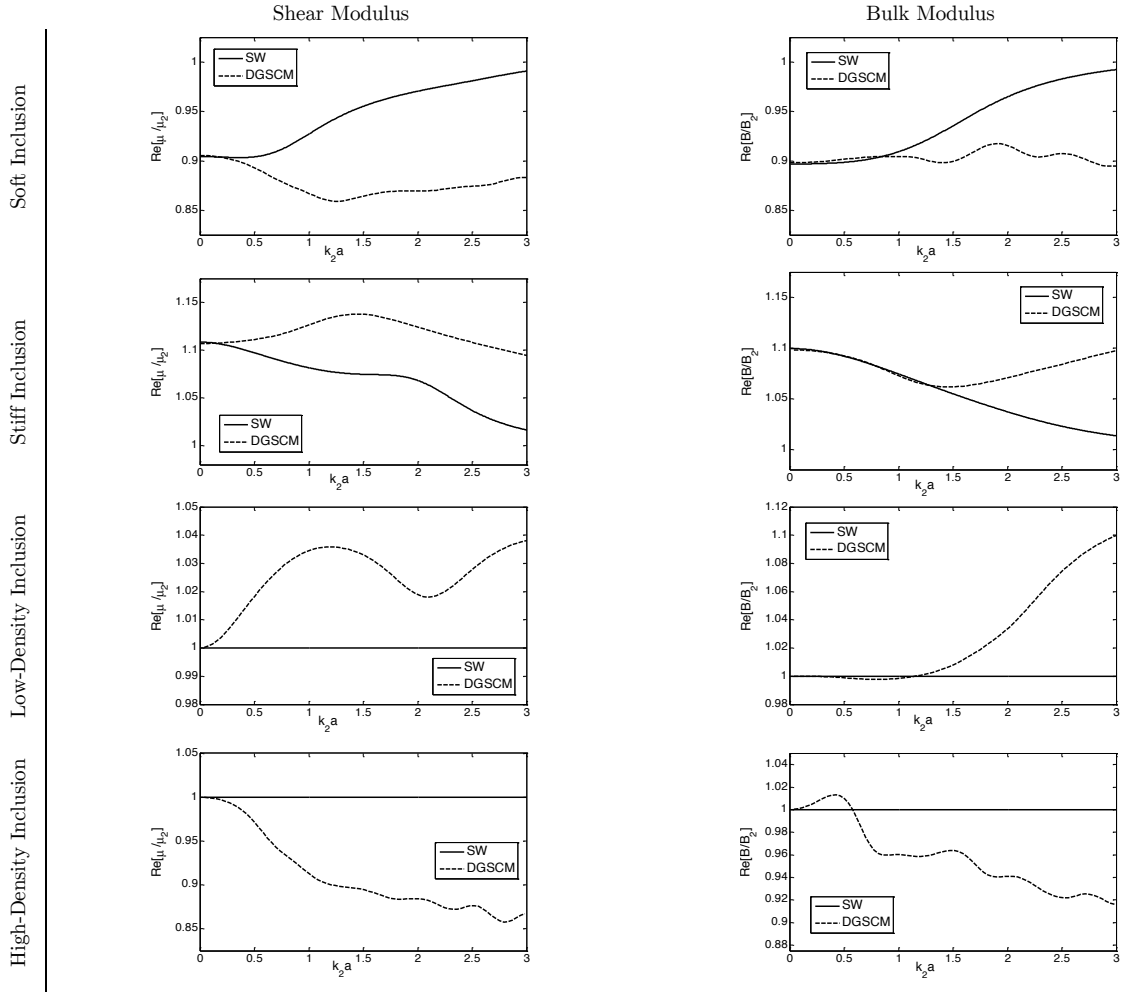

Figure 7 effective elastic constants versus dimensionless frequency predicted by DGSCM and SW models for $c = 0.15$.

Figure 8 illustrates variations of the effective dynamic properties versus volume fraction of the constituent particles. As can be seen from the figure, the DGSCM model in the composites which contain stiff particles is exactly able to predict the expected final elastic properties. For example, this model demonstrates the normalized shear modulus at $c=1$ for the composites with soft and stiff reinforcements equal to $Re[\mu/\mu_2]=0.5$ and $Re[\mu/\mu_2]=2$, respectively, which are exactly the same expected values. But in the materials containing light and heavy particles in spite of the expectation, some variations in the effective dynamic constants are seen. The reverse case is observed for the SW model.

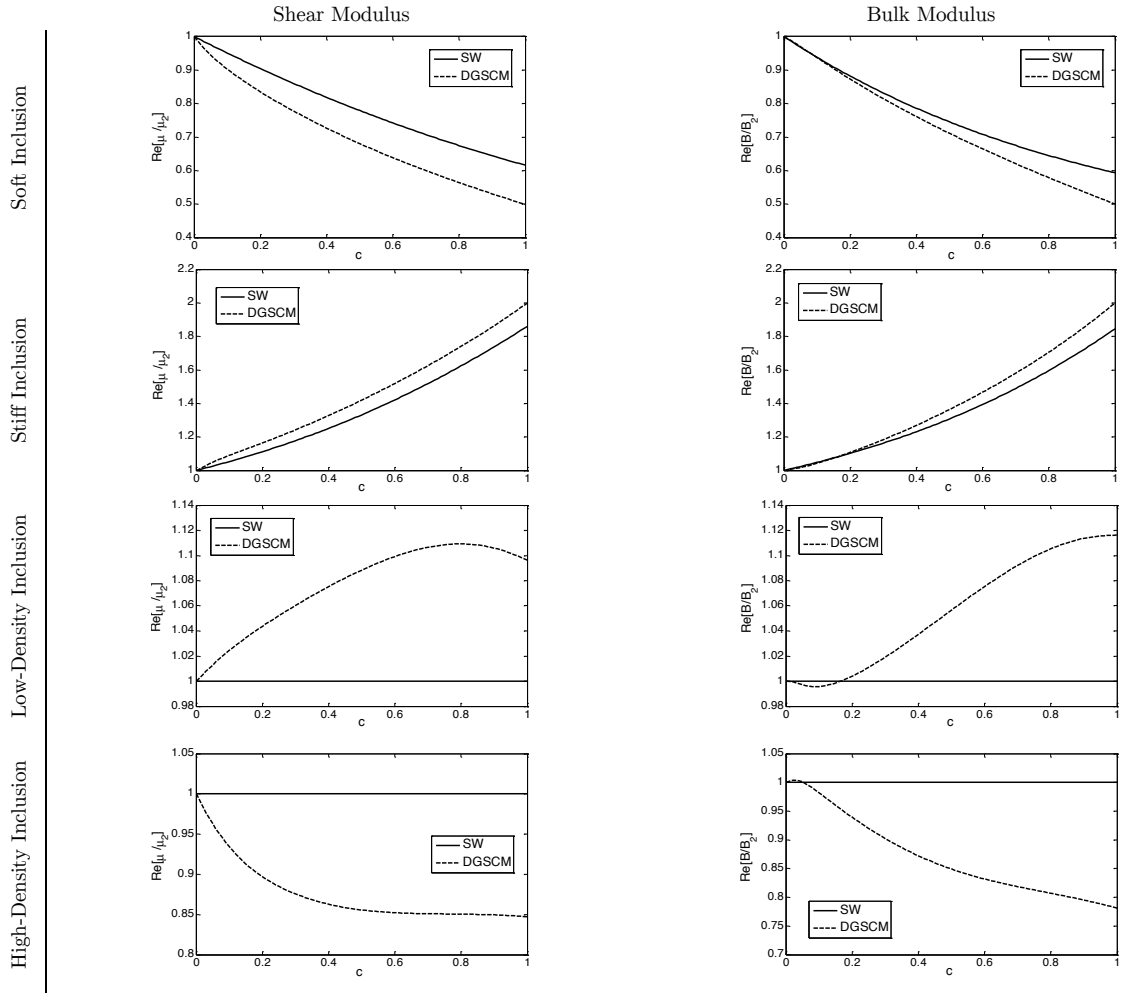

Figure 8 effective elastic constants versus volume concentration predicted by DGSCM and SW models for $k_2a=1$.

6 CONCLUSIONS

This paper aims to investigate propagation of the longitudinal elastic wave in the random particulate composites. The models of Foldy and WT were used from the set of effective field methods, while the models of SW and DGSCM were utilized from the set of effective mediums for sake of analysis and comparison. Four types of composites with different particles but the same matrix were considered. In two types of these composites, the mass density of the particles was taken equal to the mass density of the matrix, while their elastic constants were assumed to be half and twice those of the matrix accordingly. In the other two composites, elastic constants of the particles and the matrix were deemed the same, but mass density of the former was considered to be half that of the matrix one time and twice that of the matrix the other time.

Variations of the phase velocity and attenuation along with the effective dynamic properties of these composites were explored in terms of volume concentration and dimensionless wave number by using the models. It can be inferred from the obtained results that the models behavior in comparison with each other is heavily dependent on properties of the composite constituents. The mentioned methods of effective medium in comparison to the methods of effective field are more capable of predicting a more consistent behavior with the expected physical phenomena.

Meanwhile, comparing the four composite materials which were mentioned in the DGSCM model reveal some other interesting findings. The coherent attenuation in the composites containing heavy particles is considerably greater than other mentioned composites. Normalized phase velocity of the average wave provides the maximum and the minimum values in the case of using stiff and heavy reinforcements, respectively.

References

Berryman J.G. (1980). Long-wavelength propagation in composite elastic media-I. spherical inclusions, J. Acoust. Soc. Am., 68:1809-1819.

Bringi V.N., Varadan V.V., Varadan V.K. (1982). Coherent wave attenuation by a random distribution of particles, Radio Science, 17(5):946–952.

Budiansky B. (1965). on the elastic moduli of some heterogeneous materials, J. Mech. Phys. Solids, 13:223–227.

Christensen R. M. (1990). A Critical Evaluation for a Class of Micro-Mechanics Model, J. Mech. Phys. Solids, 38:379-404.

Datta S.K., Ledbetter H.M., Shindo Y., Shah A.H. (1988). Phase velocity and attenuation of plane elastic waves in a particle-reinforced composite medium, Wave Motion, 10:171-182.

Foldy L.L. (1945). The multiple scattering of waves, Phys. Rev., 67:107–119.

Hill R. (1965). A self consistent mechanics of composite materials, J.Mech. Phys. Solids, 13:213-222.

Kanaun S.K., Levin V.M., Sabina F.J. (2004). Propagation of elastic waves in composites with random set of spherical inclusions (effective medium approach), Wave Motion, 40:69-88.

Kanaun S., Levin V. (2005). Propagation of shear elastic waves in composites with a random set of spherical inclusions (effective field approach), International Journal of Solids and Structures, 42(14):3971–3997.

Kanaun S.K., Levin V.M. (2007). Propagation of longitudinal elastic waves in composites with a random set of spherical inclusions (effective field approach), Arch. Appl. Mech., 77:627-651.

Kamat S.V., Hirth J.P., Mehrabian R. (1989). Mechanical properties of particulate-reinforced aluminum-matrix composites, Acta metal, 37(9):2395-2402.

Kinra V.K., Anand A. (1982). Wave propagation in a random particulate composite at long and short wavelengths, Int. J. Solids Struct. , 18:367-380.

Kinra V.K., Ker E., Datta S.K. (1982). Influence of particle resonance on wave propagation in a random particulate composite, Mech. Res. Commun., 9:109-114.

Kinra V.K., Day N.A., Maslov K., Henderson B.K., Diderich G. (1997). The transmission of a longitudinal wave through a layer of spherical inclusions with a random or periodic arrangement, J.Mech. Phys. Solids, 46:153-165.

Kim J.Y., Ih J.G., Lee B.H. (1995). Dispersion of elastic waves in random particulate composites, J. Acoust. Soc. Am., 97:1380-1388.

Kuster G.T., Toksoz M.N. (1974). Velocity and attenuation of seismic waves in two-phase media: Part I. Theoretical formulation, Geophysics, 39:587-606.

Lax M. (1951). Multiple scattering of waves, Rev. Mod. Phys., 23:287–310.

Layman C., Murthy N.S., Yang R.B., Wu J. (2006). The interaction of ultrasound with particulate composites, J. Acoust. Soc. Am., 119:1449-1456.

Lloyd P., Berry M.V. (1967). Wave propagation through an assembly of spheres IV Relations between different multiple scattering theories, Proc. Phys. Soc., 91:678-88.

Liu D., Turner J.A. (2008). Influence of spatial correlation function on attenuation of ultrasonic waves in two-phase materials, J.Acoust.Soc.Am., 123(5):2570-2576.

Mal A. K., Bose S. K. (1974). Dynamic moduli of a suspension of imperfectly bonded spheres, Proc. Cambridge Philos. Soc., 76:578–600.

Markov K.Z., Willis J.R. (1998). An explicit formula for the two-point correlation function for dispersions of nonoverlapping spheres, Math. Mod. Meth. Appl. Sciences, 8(2):359–377.

Markov K.Z. (1999). on the correlation functions of two-phase random media and related problems, Proc. Roy. Soc. A, 1999, 455(1983):1049–1066.

Pao Y.H., Mow C.C. (1973). Diffraction of elastic waves and dynamic stress concentrations, Crane and Russak (NewYork).

Rahimzadeh M. (2013). Elastic wave propagation in nano-composites with random distribution of spherical inclusions, Latin American Journal of Solids and structures, 10(4):813-831.

Sabina F.J., Willis J.R. (1988). A simple Self Consistent analysis of wave propagation in particulate composites, Wave Motion, 10:127–142.

Sato H., Shindo Y. (2003). Multiple scattering of plane elastic waves in a particle-reinforced-composite medium with graded interfacial layers, Mech. Mater., 35:83-106.

Varadan V.K., Ma Y., Varadan V.V. (1985). A multiple scattering theory for elastic wave propagation in discrete random media, J. Acoust. Soc. Am., 77(2):375–385.

Waterman P.C., Truell R. (1961). Multiple scattering of elastic waves, J. Math. Phys., 2:512–537.

Wei P.J., Huang Z.P. (2004). Dynamic effective properties of the particle-reinforced composites with the viscoelastic interphase, Int. J. Solids Struct., 41:6993-7007.

Willis. J.R. (1980). a polarization approach to the scattering of elastic waves -I. Scattering by a single inclusion, J. Mech. Phys. Solids, 28:287–305.

Willis, J.R. (1980). a Polarization approach to the scattering of elastic waves-II. multiple scattering from inclusions, J. Mech. Phys. Solids, 28:307-327.

Yang R.B. (2003). A dynamic generalized self-consistent model for wave propagation in particulate composites, J. Appl. Mech., 70:575–582.

Ying C. F., Truell R. (1956). Scattering of a plane longitudinal wave by a spherical obstacle in an isotropically elastic solid, J. Appl. Phys., 27:1086-1097.

Appendix 1

$$Q_{71}^{(1)} = n\, j_n\left(k_2 a\right) - k_2 a\, j_{n+1}\left(k_2 a\right) \tag{A.1}$$

$$Q_{71}^{(3)} = n\, h_n^{(1)}\left(k_2 a\right) - k_2 a\, h_{n+1}^{(1)}\left(k_2 a\right) \tag{A.2}$$

$$Q_{72}^{(3)} = n\left(n+1\right) h_n^{(1)}\left(K_2 a\right) \tag{A.3}$$

$$Q_{81}^{(1)} = j_n\left(k_2 a\right) \tag{A.4}$$

$$Q_{81}^{(3)} = h_n^{(1)}\left(k_2 a\right) \tag{A.5}$$

$$Q_{82}^{(3)} = \left(n+1\right) h_n^{(1)}\left(K_2 a\right) - K_2 a\, h_{n+1}^{(1)}\left(K_2 a\right) \tag{A.6}$$

$$Q_{11}^{(1)} = \left(n^2 - n - \frac{\left(K_2 a\right)^2}{2} \right) j_n\left(k_2 a\right) + 2 k_2 a\, j_{n+1}\left(k_2 a\right) \tag{A.7}$$

$$Q_{11}^{(3)} = \left(n^2 - n - \frac{\left(K_2 a\right)^2}{2} \right) h_n^{(1)}\left(k_2 a\right) + 2 k_2 a\, h_{n+1}^{(1)}\left(k_2 a\right) \tag{A.8}$$

$$Q_{12}^{(3)} = n\left(n+1\right)\left[\left(n-1\right) h_n^{(1)}\left(K_2 a\right) - K_2 a\, h_{n+1}^{(1)}\left(K_2 a\right) \right] \tag{A.9}$$

$$Q_{41}^{(1)} = \left(n-1\right) j_n\left(k_2 a\right) - k_2 a\, j_{n+1}\left(k_2 a\right) \tag{A.10}$$

$$Q_{41}^{(3)} = \left(n-1\right) h_n^{(1)}\left(k_2 a\right) - k_2 a\, h_{n+1}^{(1)}\left(k_2 a\right) \tag{A.11}$$

$$Q_{42}^{(3)} = \left(n^2 - 1 - \frac{\left(K_2 a\right)^2}{2} \right) h_n^{(1)}\left(K_2 a\right) + K_2 a\, h_{n+1}^{(1)}\left(K_2 a\right) \tag{A.12}$$

$$W_{71}^{(1)} = n\, j_n\left(k_1 a\right) - k_1 a\, j_{n+1}\left(k_1 a\right) \tag{A.13}$$

$$W_{72}^{(3)} = n\left(n+1\right) h_n^{(1)}\left(K_1 a\right) \tag{A.14}$$

$$W_{81}^{(1)} = j_n\left(k_1 a\right) \tag{A.15}$$

$$W_{82}^{(1)} = (n+1)\, j_n(K_1 a) - K_1 a\, j_{n+1}(K_1 a) \tag{A.16}$$

$$W_{11}^{(1)} = \left(n^2 - n - \frac{(K_1 a)^2}{2} \right) j_n(k_1 a) + 2k_1 a\, j_{n+1}(k_1 a) \tag{A.17}$$

$$W_{12}^{(1)} = n(n+1)\left[(n-1)\, j_n(K_1 a) - K_1 a\, j_{n+1}(K_1 a) \right] \tag{A.18}$$

$$W_{41}^{(1)} = (n-1)\, j_n(k_1 a) - k_1 a\, j_{n+1}(k_1 a) \tag{A.19}$$

$$W_{42}^{(1)} = \left(n^2 - 1 - \frac{(K_1 a)^2}{2} \right) j_n(K_1 a) + K_1 a\, j_{n+1}(K_1 a) \tag{A.20}$$

Appendix 2

$$\mathbf{P} = \begin{bmatrix} P_{11} & P_{12} \\ P_{21} & P_{22} \end{bmatrix},\ \mathbf{Q} = \begin{bmatrix} Q_{11} & Q_{12} \\ Q_{21} & Q_{22} \end{bmatrix} \tag{A.21}$$

$$P_{11} = n h_n^{(1)}(kb) - kb h_{n+1}^{(1)}(kb) \tag{A.22}$$

$$P_{12} = n(n+1) h_n^{(1)}(Kb) \tag{A.23}$$

$$P_{21} = h_n^{(1)}(kb) \tag{A.24}$$

$$P_{22} = (n+1) h_n^{(1)}(Kb) - Kb h_{n+1}^{(1)}(Kb) \tag{A.25}$$

$$Q_{11} = (n^2 - n - \frac{1}{2} K^2 b^2) h_n^{(1)}(kb) + 2kb h_{n+1}^{(1)}(kb) \tag{A.26}$$

$$Q_{12} = n(n+1)\left[(n-1) h_n^{(1)}(Kb) - Kb h_{n+1}^{(1)}(Kb) \right] \tag{A.27}$$

$$Q_{21} = (n-1) h_n^{(1)}(kb) - kb h_{n+1}^{(1)}(kb) \tag{A.28}$$

$$Q_{22} = (n^2 - 1 - \frac{1}{2} K^2 b^2) h_n^{(1)}(Kb) + Kb h_{n+1}^{(1)}(Kb) \tag{A.29}$$

$$\Phi_{mn} = \frac{i^{n-1}}{k}(2n+1)\delta_{m0} \tag{A.30}$$

$$X_{mn} = \frac{i^{n-1}}{2K}\frac{2n+1}{n(n+1)}\left[\delta_{m1} - n(n+1)\delta_{m,-1}\right] \tag{A.31}$$

Other matrices in the equation (35) are defined via substitutions according to Table A.1.

Table A.1 Definition of the unknown matrices

	Substitute	*For*
$\mathbf{P}^{(2)},\mathbf{Q}^{(2)}$	k,K	k_2,K_2
$\tilde{\mathbf{P}}^{(2)},\tilde{\mathbf{Q}}^{(2)}$	$h_n^{(1)}$	j_n
	k,K	k_2,K_2
$\mathbf{P}^{(1)},\mathbf{Q}^{(1)}$	kb,Kb	k_1a,K_1a
$\tilde{\mathbf{P}}^{(1)},\tilde{\mathbf{Q}}^{(1)}$	$h_n^{(1)}$	j_n
	kb,Kb	k_1a,K_1a
$\mathbf{P}^{0},\mathbf{Q}^{0}$	kb,Kb	k_2a,K_2a